



*Citation for published version:*

Ding, R, Zhang, J, Xu, B, Cheng, M & Pan, M 2019, 'Energy Efficiency Improvement of Heavy-Load Mobile Hydraulic Manipulator with Electronically Tunable Operating Modes', *Energy Conversion and Management*, vol. 188, pp. 447-461. <https://doi.org/10.1016/j.enconman.2019.03.023>

*DOI:*

[10.1016/j.enconman.2019.03.023](https://doi.org/10.1016/j.enconman.2019.03.023)

*Publication date:*

2019

*Document Version*

Peer reviewed version

[Link to publication](#)

*Publisher Rights*  
CC BY-NC-ND

**University of Bath**

**Alternative formats**

If you require this document in an alternative format, please contact:  
[openaccess@bath.ac.uk](mailto:openaccess@bath.ac.uk)

**General rights**

Copyright and moral rights for the publications made accessible in the public portal are retained by the authors and/or other copyright owners and it is a condition of accessing publications that users recognise and abide by the legal requirements associated with these rights.

**Take down policy**

If you believe that this document breaches copyright please contact us providing details, and we will remove access to the work immediately and investigate your claim.

# 1 Energy Efficiency Improvement of Heavy-Load Mobile Hydraulic Manipulator 2 with Electronically Tunable Operating Modes

3 Ruqi Ding<sup>a</sup>, Junhui Zhang<sup>b\*</sup>, Bing Xu<sup>b</sup>, Min Cheng<sup>b,c</sup>, Min Pan<sup>d</sup>

4 a. Key Laboratory of Conveyance and Equipment, Ministry of Education, East China Jiaotong University, Nanchang, China

5 b. State Key Laboratory of Fluid Power and Mechatronic Systems, Zhejiang University, Hangzhou, China

6 c. College of Mechanical Engineering, Chongqing University, Chongqing, China

7 d. The Centre for Power Transmission and Motion Control, University of Bath, United Kingdom

8 **Abstract:** The conventional hydraulic drive system for a heavy-load mobile manipulator is usually operated under single mode,  
9 such that both inlet/outlet and potential energy losses are large to lower the energy efficiency. In this paper, a novel electro-hydraulic  
10 drive system is presented to improve energy efficiency. Extended control degrees of freedom are obtained utilizing the independent  
11 metering valve and electronic controlled pump. Then, multiple operating modes are carried out pertaining to the cylinder, valve, and  
12 pump. To achieve both optimal energy efficiency and precise motion tracking, both multi-mode switching and multi-variable  
13 controller are designed to accommodate with time-varying and uncertain load characteristics. As a consequence, the inlet, outlet, and  
14 potential energy losses can be decreased simultaneously. The experimental validation is conducted by using a three-joint manipulator  
15 in a 2t excavator. A duty cycle of movement including all three actuators and covering full load quadrants is used to evaluate the  
16 efficiency improvement. Compared with the conventional load sensing system, the proposed multi-mode switching system using the  
17 pump pressure with valve meter-in control mode yields a 25.8% energy-saving ratio. Furthermore, the pump flow with valve  
18 meter-out control mode yields a 35.3% energy-saving ratio. Using this combined control mode, higher efficiency can be obtained due  
19 to the minimum inlet losses, but faster dynamic response together with higher overshoot will appear. It is proved that the energy  
20 efficiency is improved, while the motion tracking performance is not degraded by introducing the multi-mode switching.

21 **Keywords:** hydraulic manipulator; energy saving; mode switching; energy regeneration; independent metering control

## 23 1. Introduction

24 Multi-DOF (Degree of Freedom) manipulators are always applied to various industrial and mobile machines. Electric  
25 drive systems are most commonly used to convert the input electric energy to potential and kinetic energies of the  
26 manipulator. However, the low power-density ratio restricts their applications in heavy-load mobile manipulators, such  
27 as an underwater manipulator, crane, construction machinery, agricultural machinery, etc. Characterized by high  
28 power-weight ratio, fast response, high stiffness, and high load capability, hydraulic drive systems have been widely  
29 applied in heavy-load manipulators. Other than the distributed control using the electric drive system, the control of the  
30 hydraulic drive system is centralized, of which multiple joints are supplied by one power unit. The coupling property  
31 among different joints makes the energy efficiency of hydraulic drive system lower than the electric one. Considering  
32 the environmental problems and economic benefit [1], tackling challenges related to energy efficiency and energy  
33 saving in heavy-load mobile hydraulic manipulators is a highly topical issue [2].

34 In a hydraulic manipulator, the hydraulic drive system converts pressure energy to potential and kinetic energies, as  
35 shown in Fig.1(a). The input mechanical energy could be provided by an electric motor or combustion engine. The  
36 pressure energy (hydraulic energy) from a hydraulic pump is distributed into multiple actuators by control valves. There

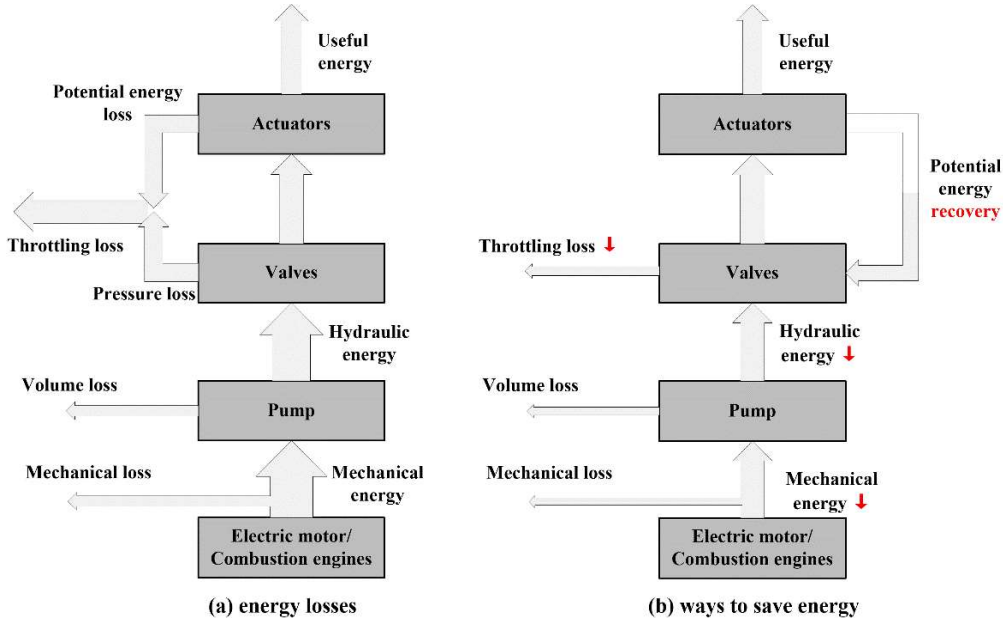
---

\*Corresponding author. Tel.: +86 571 87952505. Fax.: +86 571 87952507.  
E-mail address: [benzjh@zju.edu.cn](mailto:benzjh@zju.edu.cn) (J. Zhang).

## Nomenclature

$A_a$	Head side area of cylinder ( $m^2$ )	$\Delta p_{v2}$	pressure difference of meter-out valve (Pa)
$A_b$	Rod side area of cylinder ( $m^2$ )	$q_a$	Flow of head side chamber ( $m^3/s$ )
$B_p$	Coefficient of viscous friction	$q_b$	Flow of rod side chamber ( $m^3/s$ )
$C_p$	Leakage coefficient of pump	$q_c$	Difference between reference flow calculated flows ( $m^3/s$ )
$E_H$	Hydraulic energy (J)	$q_i$	Flow for each actuator ( $i=1,2,3$ ) (Pa) ( $m^3/s$ )
$E_p$	Energy consumption of pump (J)	$q_{i,ref}$	Reference flow for each actuator ( $i=1,2,3$ ) (Pa) ( $m^3/s$ )
$E_s$	Energy consumption of system (J)	$q_s$	Pump flow ( $m^3/s$ )
$E_{v1}$	Throttling loss of inlet (J)	$q_{s,ref}$	Reference flow for pump ( $m^3/s$ )
$E_{v2}$	Throttling loss of outlet (J)	$q_v$	Flow across valve( $m^3/s$ )
$F_L$	Load force (N)	$q_{v,lim}$	Threshold of flow across valve( $m^3/s$ )
$F_{L,lim}$	Threshold of Load force (N)	$u_v$	Control voltage of valve (v)
$K_V$	Flow-pressure coefficient of valve	$u_{v1}$	Control voltage of inlet valve 1 (v)
$K_d$	Differentiation coefficient	$u_{v2}$	Control voltage of outlet valve (v)
$K_i$	Integration coefficient	$u_p$	Control voltage of pump (v)
$K_p$	Proportion coefficient	$v$	Cylinder velocity (m/s)
$m_L$	Equivalent load mass (kg)	$v_{ref}$	Reference velocity of cylinder (m/s)
$n_m$	Rotating speed of pump (r/min)	$v_i$	Velocity of boom cylinder m/s)
$p_a$	Pressure in head side chamber (Pa)	$v_{1,ref}$	Reference velocity of boom cylinder m/s)
$p_b$	Pressure in rod side chamber (Pa)	$v_2$	Velocity of arm cylinder (m/s)
$p_c$	Pressure threshold of cavitation (Pa)	$v_{2,ref}$	Reference velocity of arm cylinder (m/s)
$p_L$	Load pressure (Pa)	$v_3$	Velocity of bucket cylinder m/s)
$p_L$	Load pressure for each actuator ( $i=1,2,3$ ) (Pa)	$v_{3,ref}$	Reference velocity of bucket cylinder (m/s)
$p_{Ls}$	Maximum load pressure (Pa)	$V_p$	Pump displacement (cc/r)
$p_m$	Pressure margin between pump and load (Pa)	$\theta_s$	Pump swivel angle (deg)
$p_{min}$	Permitted minimum chamber pressure (Pa)	$\theta_{s,max}$	Maximum pump swivel angle (deg)
$p_{ref}$	Reference pressure in rod side chamber (Pa)	$\theta_{s,ref}$	Reference pump swivel angle (deg)
$p_r$	Drain pressure (Pa)	$\eta_h$	Overall Energy efficiency of hydraulic system
$p_s$	Pump supply pressure (Pa)	$\eta_m$	Mechanical efficiency of pump
$\Delta p_v$	pressure difference across valve (Pa)	$\eta_p$	Efficiency of pump
$\Delta p_{v1}$	pressure difference of meter-in valve (Pa)	$\eta_v$	Volume efficiency of pump

38 are mainly three types of energy losses which influence the energy efficiency: mechanical and volume losses of the  
 39 pump, together with throttling losses of valves. The improvement of the pump efficiency requires the performance  
 40 matching between the load and engine [3]. Generally, a constant rotating speed of the engine is utilized, thus only the  
 41 throttling losses of the hydraulic drive system are aimed to optimize the energy efficiency. On one hand, the single  
 42 pump provides an adequate amount of oil to the lifting actuators to drive the manipulator reaching the desired position.  
 43 There are significant differences in pressure and flow among different actuators. Thus, discrepant pressure and flow  
 44 lead to pressure losses across the valve orifices. On the other hand, during the lowering of the manipulator, the potential  
 45 energy is often converted into heat in a speed-controlling valve without converting the energy back into recycling  
 46 energy. Therefore, how to regenerate dissipative potential energy and simultaneously decrease the pressure losses across  
 47 orifices are the key points to improve the energy efficiency of a hydraulic manipulator. A common approach to improve  
 48 efficiency with a conventional proportional directional valve is adapting the system pressure to the highest load pressure  
 49 [4]. In this system, both the pump and valve have only one operating mode, which loses the flexibility towards energy  
 50 recovery and decreases of pressure losses [5]. The energy efficiency is accepted only if the current highest load is  
 51 significantly lower than the maximum nominal load, yet the light load and especially gravity load still cause substantial  
 52 losses.



53

54

Fig.1 Energy conversion of the hydraulic drive system

55 Multi-mode switching is a good solution to improve energy efficiency because the operating mode could switch  
 56 flexibly to adapt changeable working conditions with low energy consumptions. Multi-mode switching has been  
 57 employed in various energy conversion systems. Liu et al. applied mode switching control to dual-evaporator  
 58 air-conditioning systems [6]. Wen designed a hybrid-mode two-phase interleaved boost converter to improve efficiency  
 59 and the power density of the fuel cell electric vehicle[7]. Wang presented hybrid control modes, including series control  
 60 mode, parallel control mode, and braking control mode, to decrease the fuel consumption of a heavy-duty electric  
 61 powertrain[8]. Solouk et al. developed a multi-mode engine of an electrified powertrain to improve fuel efficiency, of  
 62 which operation modes include HCCI, RCCI, and SI [9]. Nazih et al. introduced a turbocharger system that operates in  
 63 two different modes [10]. Therefore, the multi-mode switching is also a prominent alternative to substitute the single  
 64 mode operation in the conventional hydraulic drive system.

65 The commonly used approach is to supplement the energy regeneration system (ERS) to construct a hybrid power  
 66 system. Then the system including renewable energy, such as lowering potential energy or braking energy, can be  
 67 operated as an energy regeneration mode rather than the normal mode. There are well-known types of ERSs including  
 68 hydraulic type (e.g. accumulator), electric type(e.g. a battery or a combination with a supercapacitor, as well as an  
 69 electric motor/generator) and mechanical type (e.g. flywheel) [11]. They have been applied to various hydraulic  
 70 manipulators to save energies. For example, an ERS using an accumulator has been employed for a hydraulic crane[12].  
 71 ERSs of excavators were presented based on accumulators with a number of proportional valves [13] or switch valves  
 72 [14]. Similarly, ERSs based on accumulators were applied for the excavator applications together with a three-chamber  
 73 cylinder [15] or an asymmetric pump [16]. With respect to electric regeneration systems, a hybrid power excavator was

74 designed by integrating a supercapacitor [16]. The permanent magnet synchronous motor/generator was investigated  
75 [18] and it has been applied in the ERSs of a forklift [19] and mobile machinery [20].

76 With these regeneration approaches, the throttling losses of overrunning load (e.g. a gravity load) can be cancelled  
77 out, as shown in Fig.1(b). However, these recoverable forms of energy require extra mechanical, hydraulic or electric  
78 component. Therefore, they are only utilized for recovering the potential energy of the actuator with heaviest load (e.g.  
79 boom of excavator), not available for other light-load actuators. Light-load actuators still sometimes withstand  
80 overrunning loads and a spot of potential energy will be dissipated. Furthermore, additional energetic potentials from  
81 the reductions of pressure losses are not taken into account. Therefore, it is not enough to obtain an optimal energy  
82 efficiency of multi-actuator hydraulic manipulator only by the energy regeneration system.

83 To address the above issues, independent metering control valves were proposed to decouple the inlet and outlet such  
84 that the operating modes of valves can be extended with an electronic way. Thus, the potential energy under the  
85 overrunning load can be recovered and simultaneously part of the pressure loss under resistive load can be decreased.  
86 Eriksson summarized the feasible operating modes pertaining to different hardware layouts of independent metering  
87 control [21]. By introducing multiple modes, Lu and Yao designed energy-saving adaptive robust control of a hydraulic  
88 manipulator [22]. Choi et al. studied the energy-saving performance of excavator hydraulic systems through  
89 regeneration modes[23]. Kolks et al. proposed a smooth mode switching algorithm towards multi-mode transfers [24].  
90 Mattila et al. studied the independent metering control of a three-DOF redundant hydraulic robotic manipulator [25].  
91 The triple control modes of piston position, piston force, and chamber pressure tracking are designed [26]. Although the  
92 basic energy-saving principle and reactive mode switching with independent metering control valve are investigated,  
93 the effectiveness of pump control mode in efficiency improvement has rarely been addressed together, which restricts  
94 the further extensions of operating modes and accompanying efficiency improvement.

95 To further improve the energy efficiency, Quan et al. presented a pump flow control mode to replace the pressure  
96 control mode of load sensing pump[27], and then they introduced pressure-flow hybrid pump control modes into the  
97 independent metering system for the excavator [28]. However, the multi-mode configurations between pump and valve  
98 are not involved in, and these researches were measured by several simple actions, such that the energy-saving  
99 characteristic of independent metering control and its effectiveness in efficiency improvement are not fairly evaluated.  
100 Therefore, the efficiency improvement with multi-mode switching is still expected to enhance in the hydraulic  
101 manipulator application.

102 This study aims an in-depth analysis of the mode switching with independent metering control for efficiency  
103 improvement of the hydraulic manipulator. A novel electro-hydraulic drive system which enables extended control

104 degrees of freedom is presented by integrating independent metering valves and an electrically controlled pump.  
 105 Accordingly, the possible control modes for the cylinder, valve, and pump are all constructed. A systematical  
 106 configuration about the different operating modes is conducted and the corresponding multi-variable control approaches  
 107 are first developed. Considering the coordinate control of pump and valve, the energy-saving characteristic for a typical  
 108 duty cycle of an excavator manipulator is therefore evaluated. The energy-saving performance with the mode-switching  
 109 strategies is verified by the experimental results in comparison to the conventional hydraulic drive system.

## 110 2. Problem Statement

111 In a hydraulic drive system, the pump is used to convert mechanical energy into hydraulic energy. Its energy  
 112 efficiency is given with respect to mechanical and volumetric losses as:

$$113 \quad \eta_p = \eta_m \cdot \eta_v \quad (1)$$

114 The volumetric loss is mainly caused by the leakage which varying with the supply pressure, displacement angle and  
 115 rotating speed, so the volumetric efficiency  $\eta_v$  is given by:

$$116 \quad \eta_v = 1 - \frac{c_p p_s}{n_m v_p} \quad (2)$$

117 The input energy of the pump is given as:

$$118 \quad E_s = \int p_s q_s dt \quad (3)$$

119 Due to the constant rotating speed of the pump, the mechanical efficiency of the pump is neglected. Thus, the energy  
 120 loss of the pump is derived as:

$$121 \quad E_p = \frac{E_s}{\eta_v} (1 - \eta_v) \quad (4)$$

122 The velocity of each actuator is regulated by the control valve. Thus, inlet and outlet pressure losses are calculated as:

$$123 \quad E_{v1} = \Delta p_{v1} \cdot q_a \quad (5)$$

$$124 \quad E_{v2} = \Delta p_{v2} \cdot q_b \quad (6)$$

125 The energy efficiency of the hydraulic system is given by:

$$126 \quad \eta_h = 1 - \frac{E_{v1} + E_{v2} + E_p}{E_s + E_p} \quad (7)$$

127 Conventional electro-hydraulic control systems, for example, load sensing (LS) systems, are commonly used  
 128 hydraulic drive systems that make trade-offs between energy efficiency and steering quality, as shown in Fig.2. Firstly,  
 129 the pump is regulated in the pressure control mode with a hydro-mechanical way, where the pump is pre-set to maintain  
 130 a certain pressure margin over the load-leading meter-in valves. Therefore, the inlet pressure losses are held constantly  
 131 by the supply pressure control. Second, a proportional directional valve features meter-in and meter-out edges with  
 132 mechanical coupling through the valve spool. There is only one control signal, the spool position, to regulate the

133 actuator flow regardless of different load characteristics. Therefore, the control mode of the valve is also sole.  
 134 Furthermore, due to the mechanical coupling between the inlet and outlet in the directional control valve, the flow is  
 135 only charged into one cylinder chamber from the pump and then discharged to the tank from another cylinder chamber,  
 136 which is referred as normal mode. As shown in **Table.1**, four columns represent different operating conditions with  
 137 respect to the directions of the motion and load force. All the conditions are operated under normal modes.

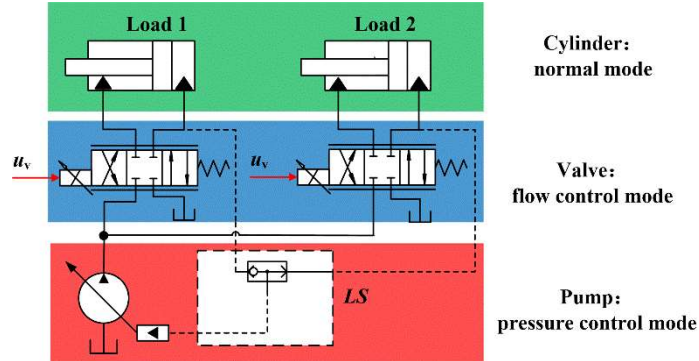


Fig.2 Conventional load-sensing system and its control mode

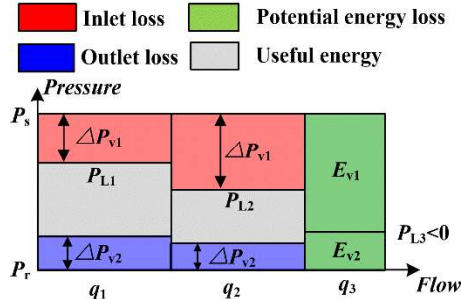
**Table.1** Single operating mode of the cylinder in the conventional system

Load condition				
Normal mode (NO)				

141  
 142 The simple control modes for the hydraulic drive system will lead to the following energy losses, as shown in **Fig.3**:  
 143 **Inlet losses:** It is mainly caused by the single mode of the pump. The pressure margin  $p_m$  is set to overcome losses  
 144 across the hoses, directional control valves and pressure compensation valves. To satisfy the requirements of all  
 145 operating points, the pump always considers the worst working conditions to preset the pressure margin, which causes  
 146 unnecessary inlet pressure losses  $\Delta p_{v1}$ . Besides, for a multi-actuator system, the system pressure is determined by the  
 147 heaviest load, such that there exists large  $\Delta p_{v1}$  in the light-load actuator due to the load difference.  
 148 **Outlet losses:** It is caused by the single mode of the valve. Due to the mechanical coupling of the inlet and outlet, the  
 149 meter-out valve cannot be operated in the pressure control mode separately. Therefore, the outlet orifice cannot open as  
 150 large as possible under resisting loads, leading to a noticeable outlet pressure loss  $\Delta p_{v2}$ .  
 151 **Potential energy losses:** It is mainly caused by the single mode of the cylinder. Under overrunning loads, the supply  
 152 flow is still required from the pump to lower loads such that the inlet energy losses  $E_{v1}$  is inevitable. Besides, the

153 potential energy cannot be recuperated and is wasted as outlet energy losses  $E_{v2}$ .

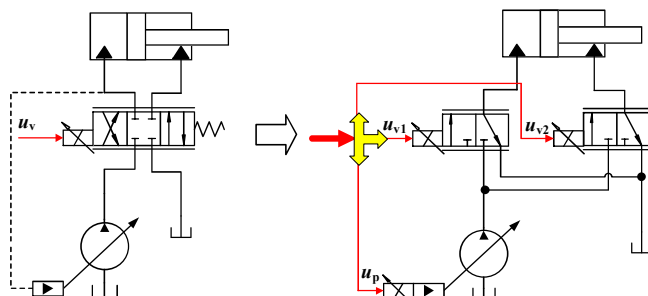
154 Due to the three aspects, the problem of low energy efficiency is serious in the conventional hydraulic system.



155  
156  
157 **Fig.3 Energy losses of the conventional system**

### 3. Electronically tunable operating modes

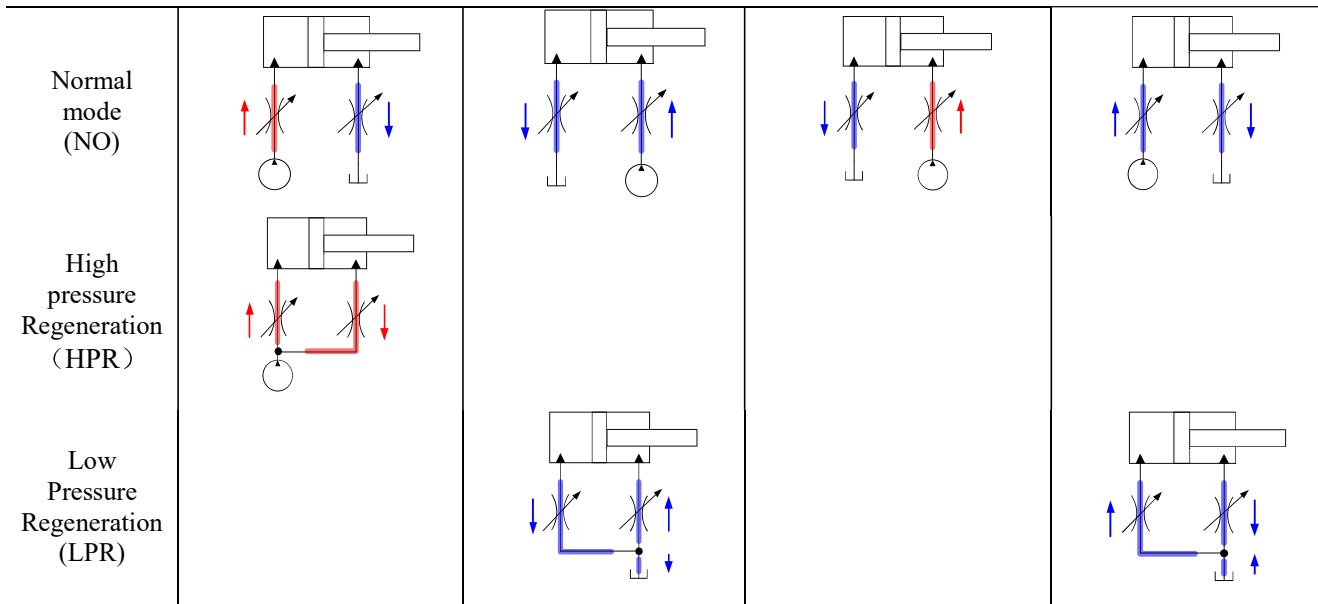
158 To improve the energy efficiency of a hydraulic manipulator, the category of operating modes should be extended  
 159 such that it can be tuned online to adapt to different load characteristics. This study designs a novel electronic-hydraulic  
 160 drive system with multiple control DOFs, as shown in Fig.4. In contrast to conventional directional valves, the  
 161 independent metering control valve is utilized which allows the individual control of meter-in and meter-out edges. The  
 162 first benefit of such decoupling controlled orifices allows individual fluid flow paths such that regeneration modes on  
 163 the low or high-pressure side are allowed. Therefore, the single normal mode of the cylinder from the high-pressure  
 164 supply to the expanding displacement volume, and from the contracting displacement volume to the low-pressure  
 165 return line can be suspended, as shown in Table.2. In HPR modes, a small load is transformed with a smaller flow and  
 166 heavy load pressure such that the inlet losses  $\Delta p_{v1}$  owing to load difference could be diminished. In LPR modes, the  
 167 gravity load has a self-generated pressure that can be pumped to cause flow such that the potential energy losses could  
 168 be diminished.



169  
170 **Fig.4 Presented electronic-hydraulic drive system based on independent metering control**

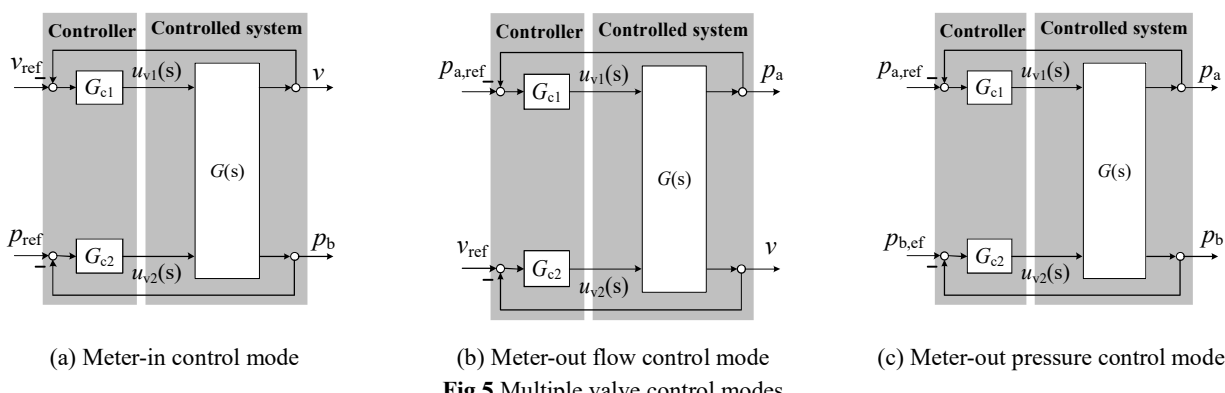
171 **Table.2 Multiple operating modes of the cylinder**

Load condition				
----------------	--	--	--	--



172

173 The second benefit of such decoupling controlled orifices is to offer a greater degree of freedom in terms of  
 174 command variables and then multiple target-variables can be controlled. Then, both flow and pressure control modes  
 175 can be achieved independently for an actuator. According to the controlled target-variables, two categories of valve  
 176 control modes are feasible containing meter-in (MI) control and meter-out (MO) control. With the meter-in control  
 177 mode, two individual control loops are designed to regulate the meter-in and meter-out areas, as shown in **Fig.5 (a)**. The  
 178 former one aims to track the required motion trajectory, while the **latter one results in** outlet losses to be as low as  
 179 possible such that the necessary supply pressure can be decreased. Due to the individual control loops of motion and  
 180 pressure, functions of the two orifices can be exchanged, which is **referred to as** meter-out control in **Figs.5 (b)** and **(c)**.  
 181 The meter-out control concept **is defined as that** the throttling losses are shifted from **the meter-in** to meter-out side.  
 182 Thus, inlet pressure losses can be decreased due to its large opening to optimize **energy efficiency**. The pressure or the  
 183 velocity of the actuator are controlled by **the** meter-out valve.



184

On the basis of decoupling controlled orifices, additional **energy-saving potentials**, which exist for inlet pressure  
 185 losses with load sensing structures, are **the further** subject of this study by using an **electrically controlled pump** in **Fig.6**.

186 A proportional directional valve together with essential pressure and swivel angle sensors is used to eliminate  
 187 conventional hydro-mechanical structure. Both supply flow and pressure control modes can be achieved in an electronic  
 188 way. Under the pump pressure (PP) control mode, the inlet pressure losses can be reduced by online tuning of the preset  
 189 pressure margin  $p_m$  to adapt to the operating conditions. However, the pressure margin  $p_m$  is unable to be set perfectly  
 190 because of the uncertainty of pressure drops across the pipelines and valves. Therefore, the preset pressure margin is  
 191 always higher than the actual demand, and unnecessary inlet pressure losses still exist. In addition, the closed-loop  
 192 pressure control is highly possible to encounter with poor dynamic issues. Under the pump flow (PF) control mode, the  
 193 swivel angle is subsequently regulated in terms of the operator's command inputs [29]. With this open-loop control  
 194 strategy, the inlet pressure loss between the pump and actuator is given by the resistance of pipelines and valves, rather  
 195 than a preset pressure margin  $p_m$ . Besides, the poor dynamic issues due to the closed-loop pressure control can also be  
 196 cancelled out. However, the issue of mismatching between supply and valve flows may lose accuracy or even rapidly  
 197 rise supply pressure to enlarge energy losses.

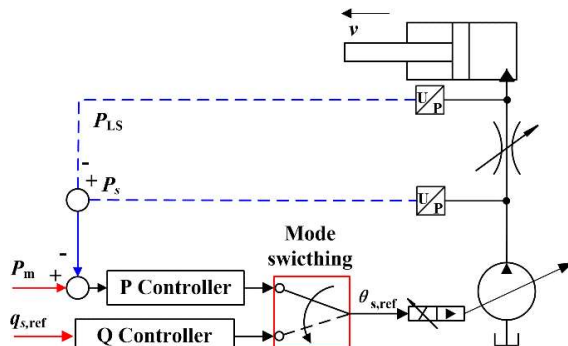


Fig.6 Dual control modes of pump

198 In a summary, because multiple modes can be tuned for both cylinder, valve and pump, there is a significant capacity  
 199 to improve energy efficiency. The challenges are configuring different modes to obtain optimal efficiency and  
 200 controlling such a system to comply with different modes by one multi-variable control system.

#### 203 **4. Efficient Mode Switching**

204 The operating modes of cylinder primarily take the load characteristics into account. Accordingly, modes  
 205 configurations among cylinder, valve and pump are then discussed based on the switching of cylinder modes.

##### 206 **4.1 Mode switching of the cylinder**

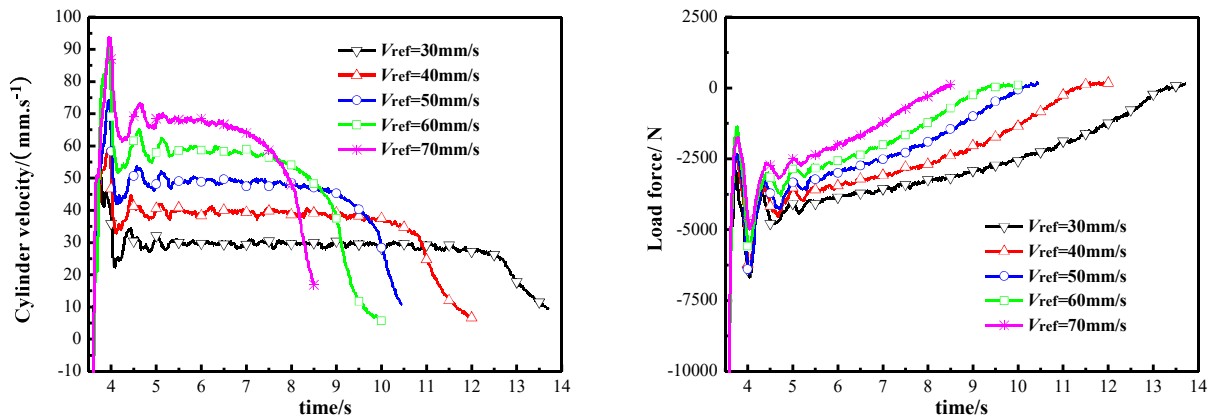
207 For the operating modes of the cylinder, a logic control that recognizes the possibility for energy regeneration is  
 208 established. A mode switching should occur when another mode is considered to be more efficient or the mode  
 209 capability is no longer sufficient. Mode capability is usually taken into account for regeneration modes by operation  
 210 limits. Operation limits emerge either through cavitation, defined by a minimum pressure threshold, or by valve stroke  
 211 limitation. There are two limitations affecting their capability:

212 **Force limitation of potential energy regeneration**

213 When lowering a gravity load, both cylinder chambers are connected to the tank under LPR mode, and the load has a  
 214 self-generated pressure that can be pumped to cause flow. As the manipulator moves down, the gravity load may  
 215 decrease until it cannot overcome the friction, inertia force, and back pressures. **Fig.7** exhibits the movement of a  
 216 cylinder driven by its gravity load. All measurements pertaining to different velocities demonstrate that the cylinder will  
 217 tend to stop when the gravity load decreases to a threshold. The threshold represents a force limitation when LPR  
 218 modes must be switched out. It is calculated according to the force balance equation as **Eq. (8) or (9)**.

219  $m_L \dot{v} = F_{L,lim} + p_a A_a - p_b A_b - B_p v$  (8)

220  $m_L \dot{v} = F_{L,lim} + p_b A_b - p_a A_a - B_p v$  (9)



221 **Fig.7** Experimental results of potential energy regeneration for excavator arm extension

221 **Flow Limitation of potential regeneration**

222 To recuperate the potential energy, the supply flow is switched from pump to suction from **the tank** under LPR mode.  
 223 However, the flow from the tank should also cross pipelines and valve orifices with a certain pressure loss. If the  
 224 pressure loss exceeds the low-level drain-line pressure, the inlet chamber would encounter with cavitation. Hence, the  
 225 LPR mode can be enabled and disabled according to **how much flow is available in the drain line**. The information on  
 226 how much flow pertaining to the valve throttling characteristics can be approximately estimated as:

227  $q_{v,lim} = K_v \sqrt{p_r - p_c}$  (10)

228 To avoid cavitation under LPR modes, the drain-line pressure should be enhanced to expand **the operating range** of  
 229 the potential energy regeneration. A simple way of doing so is to have an electrically controlled relief valve or check  
 230 valve in the return line. In this study, a check valve with 0.2 MPa cracking pressure is mounted before the tank such that  
 231 the operating ranges of LPR modes can be enlarged, as shown in **Fig.8**.

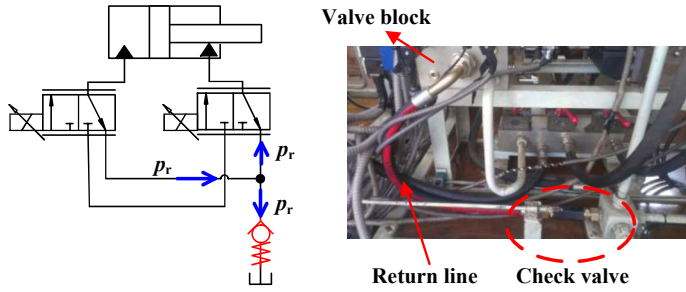


Fig.8 Enhanced tank pressure by a check valve

Taking the operation limits into account, the cylinder mode is selected according to the load quadrants, which are defined by the four combinations of the axial directions of load force and actuator velocity (shown in Fig.9). In view of the energy efficiency, the LPR mode has higher priority than the normal one when there exist overrunning loads (*Qua.II* and *Qua.IV*) unless the cylinder encounters with force or flow limitations. If so, the LPR mode has to switch to the normal one to track the required motion. Under the resistive load, the normal mode has a higher priority for the heavy load. If there exists a light resistive load, HPR mode is recommended to reduce the supply flow.

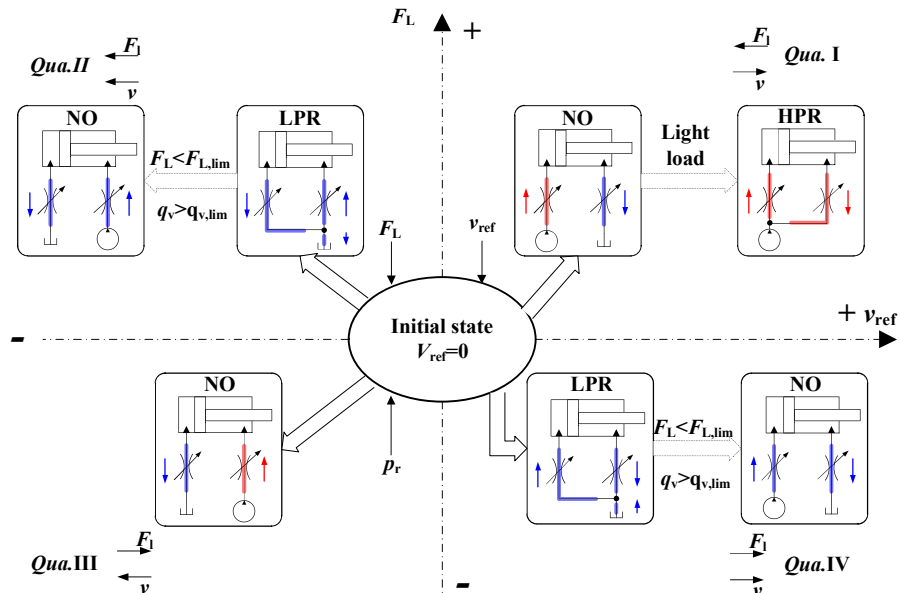


Fig.9 Cylinder mode selection for the four-quadrants load

240  
241

#### 4.2 Modes Configurations among cylinder, valve, and pump

243 To take advantages of energy regenerations to improve the efficiency, the operating modes of the cylinder are  
244 dominant compared with modes of valve and pump. It means that the configurations of valve and pump modes should  
245 comply with the selections of cylinder modes.

246 Under the overrunning loads, the actuator may be out of control to fall down rapidly, and the supply flow from pump  
247 or tank would be possible to encounter with cavitation when the valve utilizes MI control mode. Therefore, the MO  
248 valve control mode must be selected in these cases. If all the operating conditions are not beyond the mode capability,  
249 then regeneration modes are selected in the cylinder and the pump runs with the idling state (PI mode). Otherwise, the

250 cylinder still works under the NO mode, and PP control mode is a better selection for the pump because the cylinder  
 251 pressure can be directly controlled by the pressure feedback to avoid cavitation. The mode configuration for  
 252 overrunning loads is depicted in **Figs.10(a) and (b)**.

253 Under the resistive loads, both the two optional categories of valve control modes can be employed. There are two  
 254 feasible combinations of valve and pump modes, as depicted by the red and blue lines in **Fig.10(c)**. The first one utilizes  
 255 meter-in valve control together with pump pressure control (PP\_MI), and the other one utilizes meter-out valve control  
 256 together with pump flow control (PF\_MO). Meter-in valve control is not suited to pump flow control due to the  
 257 potential problem of overmatching between the supply flow and valve orifice flow.

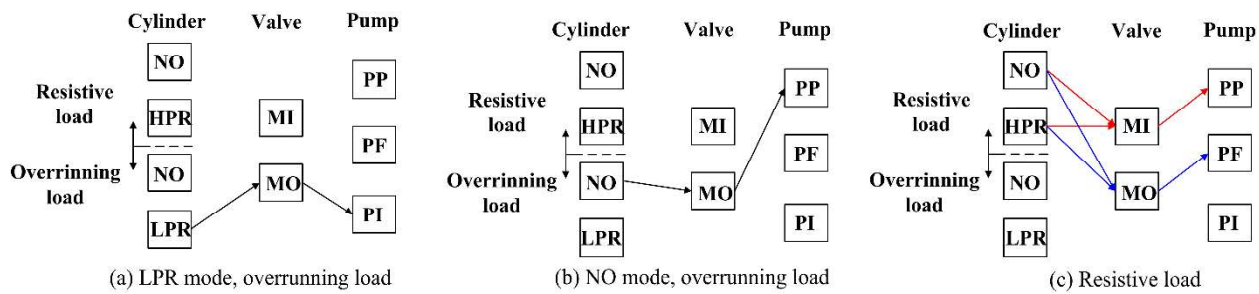


Fig.10 Mode configuration among cylinder, valve, and pump

258 In the framework of multi-mode configurations, the energy-saving capability pertaining to different load  
 259 characteristics is enhanced compared with the conventional hydraulic drive system. However, both two objectives of  
 260 optimal energy efficiency and precise motion control should be further carried out by the multi-variable controller.

## 261 5. Multi-variable control design

262 Due to the distinguishing feature between the resistive load and overrunning load, the multi-variable controllers are  
 263 designed separately for the following two conditions.

### 264 5.1 Multi-variable controller under resistive loads

265 The difference between the PP\_MI and PF\_MO modes can be captured by the multi-variable control approaches, as  
 266 shown in **Fig.11**. PP\_MI mode employs a three-input and three-output (TITO) controller. The supply pressure is  
 267 regulated beyond the load pressure by the preset pressure margin  $p_m$ . MI valve controllers are designed as: the meter-in  
 268 valve controls the input actuator velocity to distribute the supply flow, and meter-out valve controls the reference  
 269 backpressure to reduce the outlet pressure loss and simultaneously avoid the cavitation. In contrast, PF\_MO mode  
 270 employs a dual-input and triple-output controller (DITO) without the pressure margin input. The pressure feedback is  
 271 cancelled out and the supply flow is regulated according to the input velocities of all actuators. The meter-in valve is  
 272 endeavored to decrease the inlet pressure losses and the flow or pressure of each actuator is controlled by the meter-out  
 273 valve. Next, the detailed multi-variable controllers for PP\_MI and PF\_MO modes are designed in **Fig.12**.

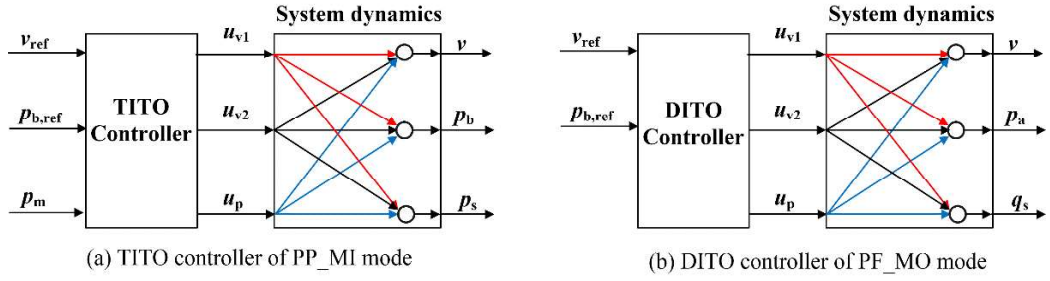
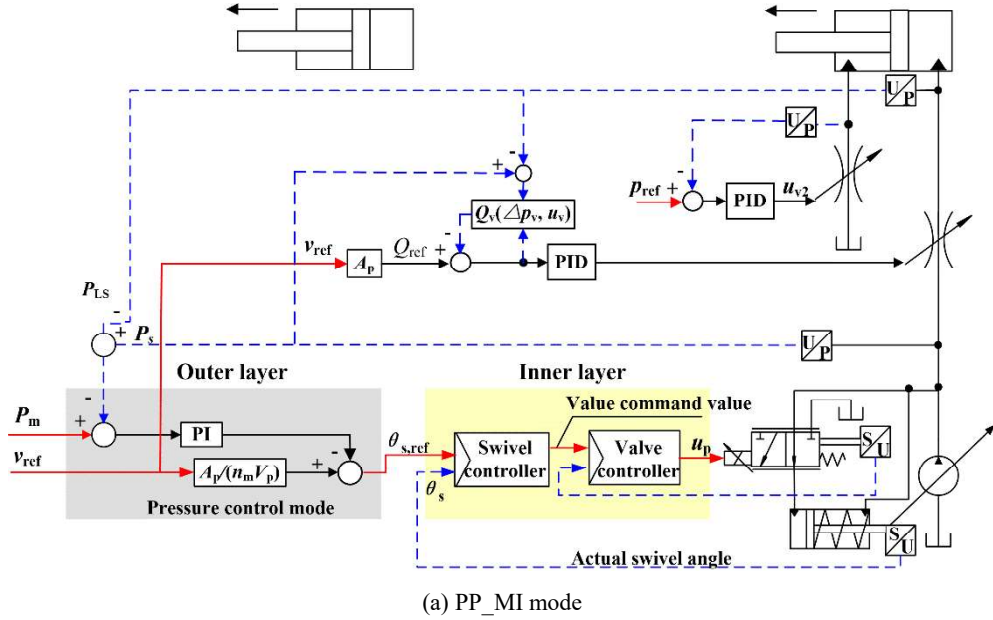
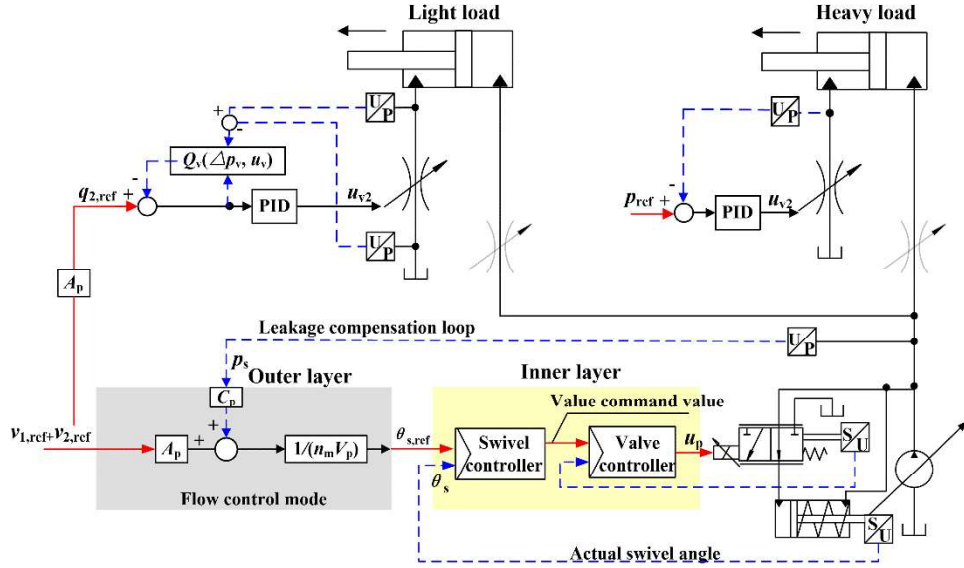


Fig.11 Multi-variable control block diagrams



(a) PP\_MI mode



(b) PF\_MO mode

Fig.12 Multi-variable control under resistive loads

274 The pump controller contains two layers. An inner layer controller consisting of valve and swivel controllers are used  
 275 to regulate the pump displacement with the feedbacks of swivel angle and valve position. The reference swivel angle to  
 276 the inner layer controller is calculated by an outer layer. PP and PF control modes of the pump are implemented in the  
 277 outer layer. PP controller includes a PI regulator to track the reference pressure margin. However, the pump dynamic

278 depends on the PI parameters, which will encounter poor response and instability. To decrease dependence of PI  
 279 parameters and improve the pump dynamic, a feedforward block to calculate the theoretical swivel angle is added such  
 280 that only a smaller output of PI regulator around the reference signal of swivel angle is required. PF controller only uses  
 281 the feedforward block as the primary method to determine the swivel angle and eliminate the pressure feedback loop.  
 282 This feedforward block utilizes a mapping from pump flow to swivel angle by applying Eq. (11), of which supply  
 283 pressure and rotate speed are included. This arrangement can **compensate for** the leakage flow with respect to the swivel  
 284 angle and pump pressure.

$$285 \quad u_p = \frac{\theta_{s,ref}}{\theta_{s,max}} = \frac{\sum q_{i,ref} + c_p p_s}{n_m v_p} \quad (11)$$

286 The valve controller contains two loops: velocity and pressure control loops, which are both designed based on the  
 287 pressure feedbacks. A calculated flow feedback controller is employed to implement **velocity tracking**. Taking PP\_MI  
 288 mode for instance [Fig.12(a)], the control signal of the meter-in valve is given by a PID regulator based on the  
 289 difference  $q_e$  between the reference flow  $q_{ref}$  and the actual one  $q_v$ .

290 Generally, the actual flow  $q_v$  is calculated utilizing a non-linear flow mode of the valve orifice in Eq. (12). The flow  
 291 **model** has been calibrated off-line as a hydraulic conductivity coefficient  $K_v$ :

$$292 \quad Q_v = K_v(u_v, \Delta p_v) \sqrt{\Delta p_v} \quad (12)$$

293 where the hydraulic conductivity coefficient  $K_v$  is subject to spool displacement, temperature and pressure difference. The  
 294 calculated flow feedback controller eliminates the non-linear dependency of load pressure such that the cylinder is able  
 295 to precisely track the reference velocity under uncertain and time-varying loads.

296 In terms of the pressure difference  $p_{b,c}$  between reference one  $p_{ref}$  and actual one  $p_b$ , the closed loop pressure control is  
 297 also implemented by means of PID regulator to reduce the outlet pressure loss. Here  $p_{ref}$  refers to the minimum **pressure**  
 298 **resisting cavitation**.

299 It is noted that under PF\_MO mode, the meter-in valves for all the actuators are opened fully to obtain the lowest  
 300 inlet pressure losses. How to achieve precise motions for different actuators is another question when there are only  
 301 meter-out valves under control. As shown in **Fig.12(b)**, the heavy load in the system uses meter-out pressure control to  
 302 reduce the supply pressure, and light loads and other loads under non-normal modes (LPR or HPR modes) are operated  
 303 by meter-out flow control to distribute the supply flow. The flow of the heavy load is determined by the subtraction  
 304 between regulated supply flow and light load flows. This measure also eliminates the over-matching problem with the  
 305 pump PF mode because excessive supply flow can be accepted by the heavy load.

## 306 5.2 Multi-variable controller under overrunning loads

307 The detailed multi-variable controller under overrunning loads are described in **Fig.13**. Under the regeneration mode,

308 the motion of the actuator is tracked by the meter-out valve. The meter-in valve is also forced to open fully. The  
 309 measure has two positive effects. The inlet pressure losses are decreased as much as possible, and the ability to resist  
 310 cavitation is also enhanced. If the operating condition is beyond the mode capability, the normal mode is switched on,  
 311 and the cylinder pressure is endeavored to track the reference value 0.3 MPa with a pump pressure controller such that a  
 312 chamber pressure beyond the threshold of cavitation is guaranteed.

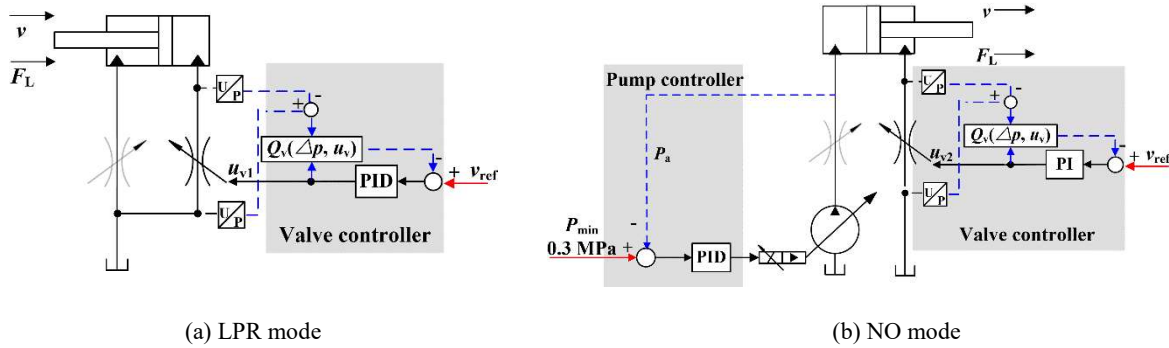


Fig.13 Multi-variable control under overrunning load

## 313 6. Energy-saving analysis

314 According to the designed mode switching and multi-variable control systems, energy consumptions using different  
 315 mode switching approaches are analyzed in a three-actuator condition. The assumption is made that all the operating  
 316 conditions are not beyond the mode capability. As shown in Fig.14, Load 1 is defined as the heavy resistive one, Load 2  
 317 is defined as the light resistive one and Load 3 is defined as a lowered gravity one. According to the logic control in  
 318 Fig.9, the cylinder modes of the three loads are NO, HPR and LPR respectively.

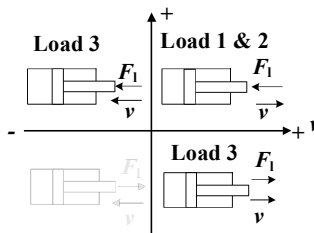


Fig.14 The distributions of three loads

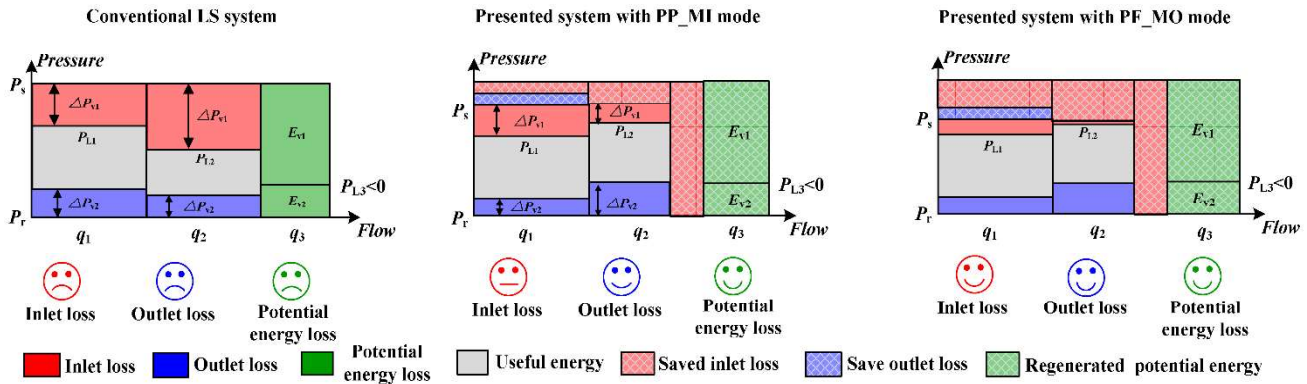
319  
 320 For Load 1 located in *Qua.I*, the outlet pressure losses of both PP\_MI and PF\_MO mode are decreased compared  
 321 with the conventional system due to the decoupling of inlet and outlet. The inlet pressure losses with PP\_MI mode can  
 322 also be reduced by diminishing the pressure margin. Compared with PP\_MI, inlet pressure losses with PF\_MO is given  
 323 by the resistance in the hoses and fully opened the meter-in valve, which can be further decreased to a minimum level.  
 324 Therefore, the system pressures of both PP\_MI and PF\_MO mode are decreased in terms of pressure losses.

325  
 326 Although located in *Qua.I*, Load 2 is changed to HPR mode both with PP\_MI and PF\_MO modes because it is the  
 327 lower load compared with Load 1. Therefore, both the head and rod sides are charged and discharged by pressure oils.

328 With a decrease of supply flow into Load 2, the energy consumptions are reduced compared with the conventional  
 329 system. Apart from the decreased flow, due to the decrease of supply pressure, another energy-saving way comes from  
 330 the diminution of inlet losses caused by the difference between Load 1 and Load 2.

331 Owing to the location in *Qua.II* or *Qua.IV*, Load 3 is changed to LPR mode. It is driven by making use of the  
 332 lowering load without any supply flow from the pump, so the energy consumptions of Load 3 are completely omitted  
 333 compared with the conventional system. In this case, there are no further improvements in energy efficiency using  
 334 PF\_MO compared with PP\_MI.

335 In a summary, the energy-saving performance in contrast to the conventional system is exhibited in **Fig.15**. Both  
 336 PP\_MI and PF\_MO modes have prominent advantages on decreases of the outlet and potential energy losses by the  
 337 flexible transfer of operating modes. Additionally, PF\_MO mode has higher efficiency than PP\_MI mode because of  
 338 further improvements of inlet pressure losses.

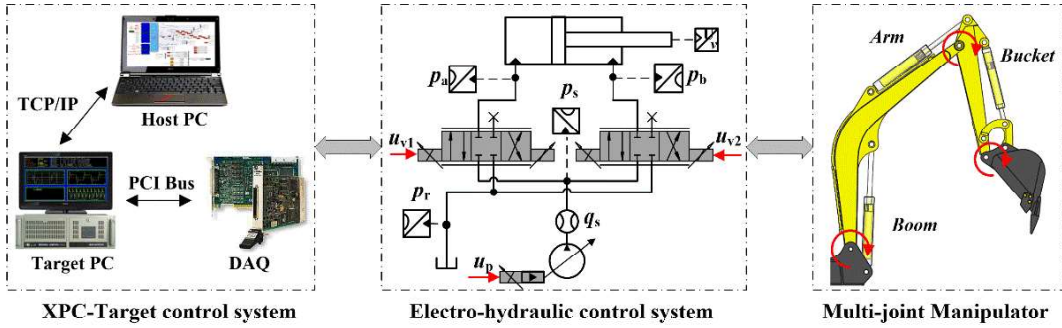


339 340 **Fig.15** Energy efficiency analysis of multi-mode switching

## 341 **7. Measurement System**

342 To have a good knowledge of working performance and energy efficiency with the tunable operating modes, a  
 343 heavy-load hydraulic manipulator of 2-ton excavator with three DOFs is studied as an example in this paper. Its  
 344 hydraulic drive system consists of proportional directional valves (PDV) and an electrically controlled pump, in which a  
 345 general system structure featuring a maximum control DOF is constructed, as shown in **Fig.16**. Two PDVs feature two  
 346 variable orifices per cylinder displacement volume: one high-pressure valve and one low-pressure valve each.  
 347 Additionally, multiple control modes of the pump are considered by means of the electrically controlled pump. Feasible  
 348 pressure and flow control modes can be differentiated by the availability of control software. To determine the operating  
 349 modes by control software, pressure sensors of four ports for an actuator are mounted. Velocity/displacement sensors, as  
 350 well as a supply flow meter, are also included to measure the system states but not used in the controller. The digital  
 351 control system is developed under the XPC Target Real-time Workshop containing a host and a target computer. The  
 352 real-time signal acquisition and control applications are both carried out on the MATLAB/Simulink software platform.

353 Main parameters of the measurement systems are listed in the following **Table.3**.



354  
355  
356

**Fig.16** Structure of measurement system

**Table.3** Descriptions of the experimental setup

Component	Specifications
Proportional directional valve	Rexroth 4WREE10E50
Electronic controlled pump	Rexroth SYDFFEE-2X/045R-PPA
Boom cylinder	0.07 m (head diameter)/0.04 m (rod diameter)/ 0.411 m (stroke)
Arm cylinder	0.07 m (head diameter)/0.04 m (rod diameter)/ 0.4 m (stroke)
Bucket cylinder	0.06 m (head diameter)/0.035 m (rod diameter)/ 0.375 m (stroke)
Electric motor	ABB QABP180L,22kw B35 380V/50HZ 4P
Data Acquisition (DAQ) Card1	NI PCI-6229
Data Acquisition (DAQ) Card2	NI PCI-6713
Pressure sensor	CYB100-20 (4-20mA, 0-20MPa, 24VDC supply)
Velocity sensor	MTS RPS 0440M D60 1 A41
Flow sensor	VSE-VS1 (Flow range: 0.05-80 L/min)

357 For this experimental measurement, the uncertainty analysis should be evaluated to capture the error range of a  
358 measured parameter [30]. The Schultz and Cole method for uncertainty analysis was utilized. Assuming that an indirect  
359 measurement combines a series of direct measurements, the compound uncertainty  $\Delta R$  is given as [31]:

$$360 \quad \Delta R = \left[ \sum_{i=1}^n \left( \frac{\partial R}{\partial x_i} \Delta x_i \right)^2 \right]^{1/2} \quad (13)$$

361 where  $\Delta R$  is the compound uncertainty,  $\Delta x_i$  ( $i=1,2,3, \dots, n$ ) is the error of each direct measurement.

362 Uncertainties of the measurement components are listed in **Table 4**. In this paper, cylinder velocities, pressures and  
363 flows are measured directly by the XPC-Target control system. The hydraulic power or energy are calculated by the  
364 multiplication of the supply flow and pressure, as exhibited in Eq. (3). Therefore, the relative uncertainties of these  
365 parameters are calculated in **Table 5**.

366 **Table.4** Uncertainties of the measurement components

Components	Measurement accuracy
Pressure sensor	0.25%
Velocity sensor	0.5%
Flow sensor	0.3%
Analog input of DAQ Card	0.016%
Signal procession module between DAQ cards and sensors	0.1%

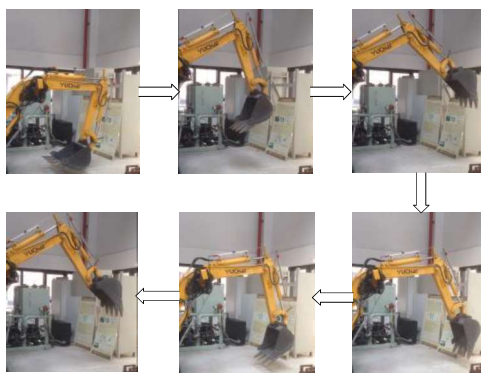
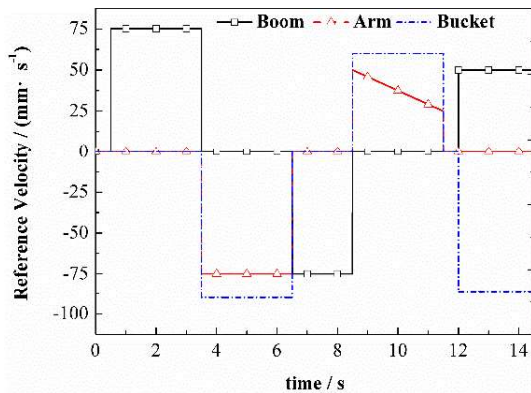
**Table.5** Relative uncertainties of experimental parameters

Parameters	Relative uncertainty
Pressure	0.270%
Velocity	0.51%
Flow	0.317%
Hydraulic Power	0.416%

## 368 8. Case Study

369 To analyze the **energy-saving potentials** that emerge through flexible operating modes, a **duty cycle** that puts as many  
 370 **technical challenges as possible** should be selected. In this paper, a continuous duty cycle involving all the three actuators  
 371 is measured in **Fig.17**. The set trajectory of each actuator is **depicted** in **Fig.18**. The cycle lasts for about 15 seconds and  
 372 includes a series actions simulating the manipulator lifting the three actuators, lowering the boom, retracting the bucket to  
 373 scoop up material, moving out from the pile, forwarding to a dump truck and unloading the material from an unloading  
 374 position.

375 Three different systems are evaluated by this duty cycle. The present hydraulic drive system with **PP\_MI** and **PF\_MO**  
 376 modes are both measured compared with the **convention load sensing (CLS) system**. The pump displacement in the  
 377 **CLS** system is regulated with a pressure control way to simulate the conventional hydro-mechanical load sensing  
 378 mechanism. The pressure margin between supply and load pressures is set to a constant **value** of 1.2 MPa in the **CLS**  
 379 system.

**Fig.17** Studied duty cycle of the measurement machine**Fig.18** Reference velocity of three actuators

380 The cylinder modes for different **actuators** are marked with different fill patterns, as shown in **Fig.19**. During the time  
 381 range of 8.5s to 11.5s, both the arm and bucket retract under overrunning loads. However, only the load of the **bucket**  
 382 **has insufficient capability** to drive the movements. Therefore, the mode of arm **switches** to LPR one, but the mode of  
 383 bucket still **switches** to the **normal one**. When the boom is lowering down, the **normal modes** in the **CLS** system is  
 384 **obviously switched** to LPR modes in the present system due to the large gravity load. **The velocity tracking errors are**  
 385 **depicted** in **Fig.20**.

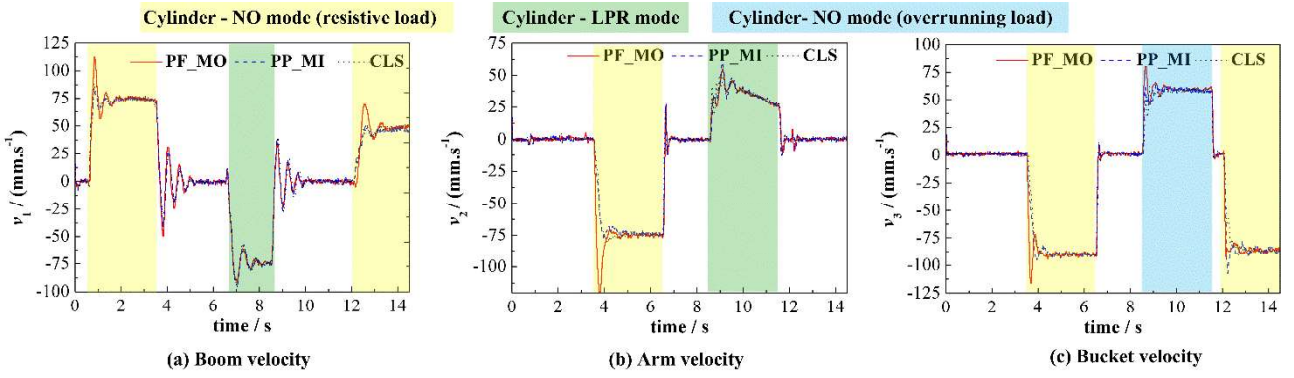


Fig.19 Comparision of motion tracking performance

Very good motion tracking can be obtained for all three hydraulic drive systems referring to Figs.19 and 20. The velocity dynamics of PP\_MI is almost the same with CLS. Compare with PP\_MI and CLS system, faster velocity response together with higher overshoot can be observed in PF\_MO under NO modes. Such higher overshoot is caused by the abrupt maximum opening of the meter-in valve rather than a low stability margin. Actually, the stability of PF\_MO is better than the other two hydraulic drive systems because of the open-loop controller. It can be confirmed that both the velocity and pressure of PF\_MO rapidly decay to a steady value. Static errors of velocity trackings are consistent. In a summary, the motion tracking performance is not degraded by introducing the multi-mode switching.

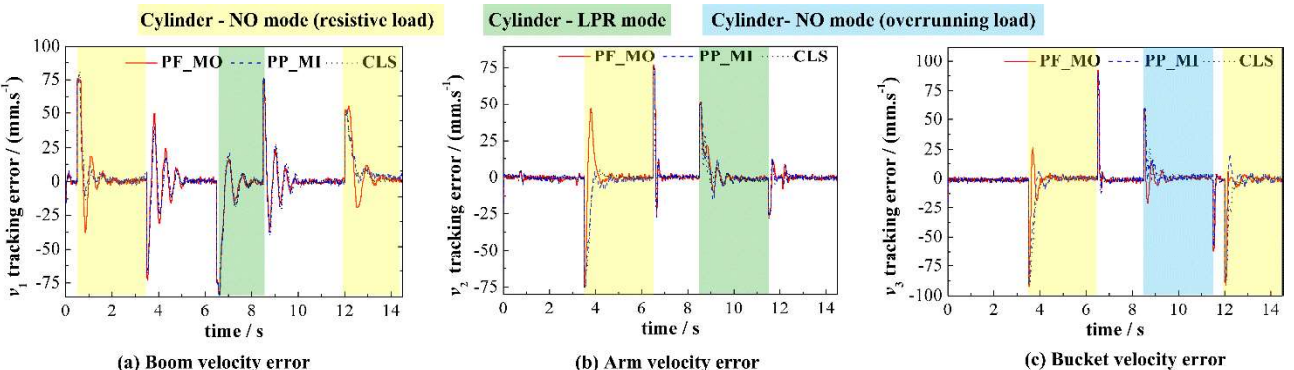


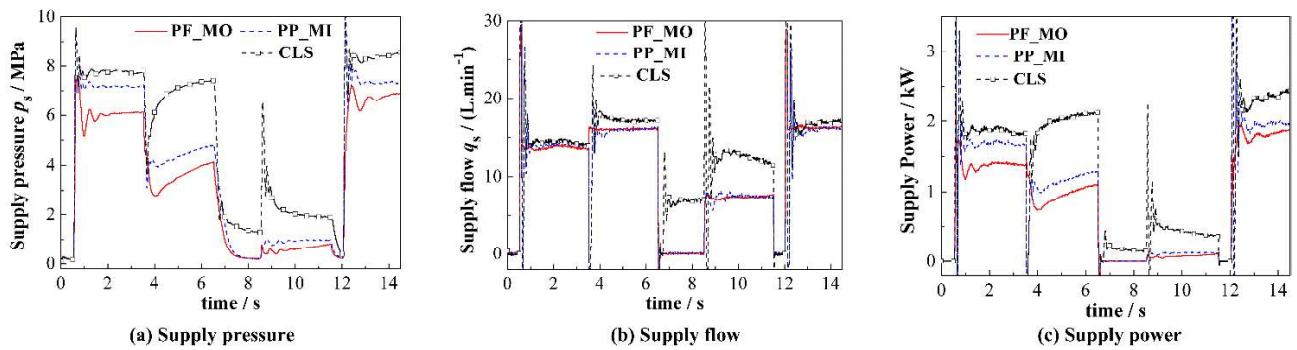
Fig.20 Comparision of velocity tracking errors

In Fig.21(a), the supply pressures of PF\_MO, PP\_MI and CLS systems are trending down in turn for an arbitrary time. Under NO modes, the decreases in supply pressure, on one hand, arise from the decreases of outlet pressure losses. It can be captured in Figs. 22 and 23 that the backpressures of the boom (0.5s~3.5s and 12s~14.8s), arm (3.5s~6.5s) and bucket (8.5s~11.5s) are only 0.3 MPa, which is approximatively 0.9 MPa in the CLS system (Fig.24). On the other hand, the optimal pressure margins using the electrically controlled pump also contribute to the reductions of supply pressures. The pressure margins of PP\_MI is decreased to 0.6 ~1.0 MPa according to the flow variations. The supply pressure of PF\_MO is further decreased compared with PP\_MI because the pressure margins achieve only 0.25 MPa by the combination of pump flow control and meter-out valve control. With respect to potential energy regeneration periods (6.5s~11.5s), the supply pressures are of course decreased because supply flows are not required from the

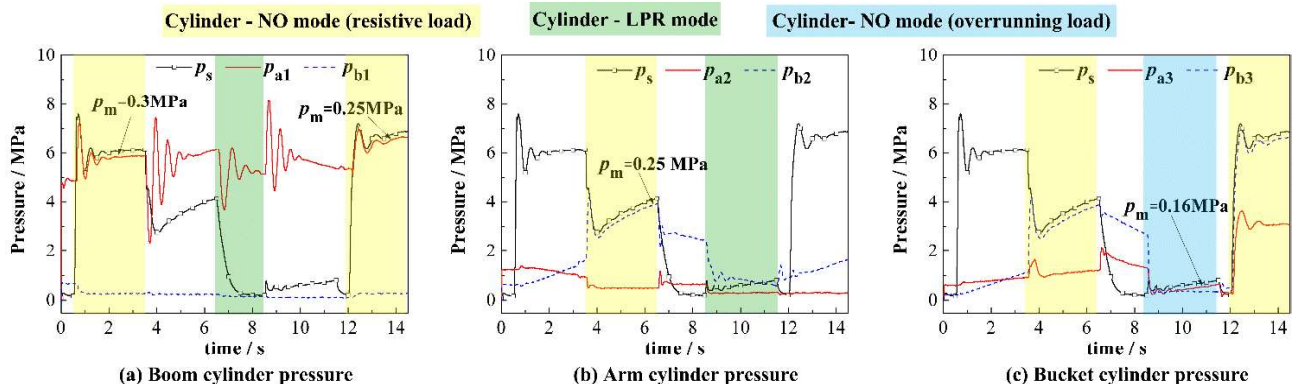
406 pump.

407 In **Fig.21(b)**, the supply flows of PF\_MO, PP\_MI and CLS systems are also trending down for an arbitrary time. The  
 408 tendency is obvious when potential energies are recuperated because the supply flows of PF\_MO and PP\_MI come  
 409 from the tank rather than the pump. Under NO modes, there is no flow regeneration from the tank. In spite of this, slight  
 410 decreases of supply flow still exist because less pump volume losses are obtained by lower supply pressures.

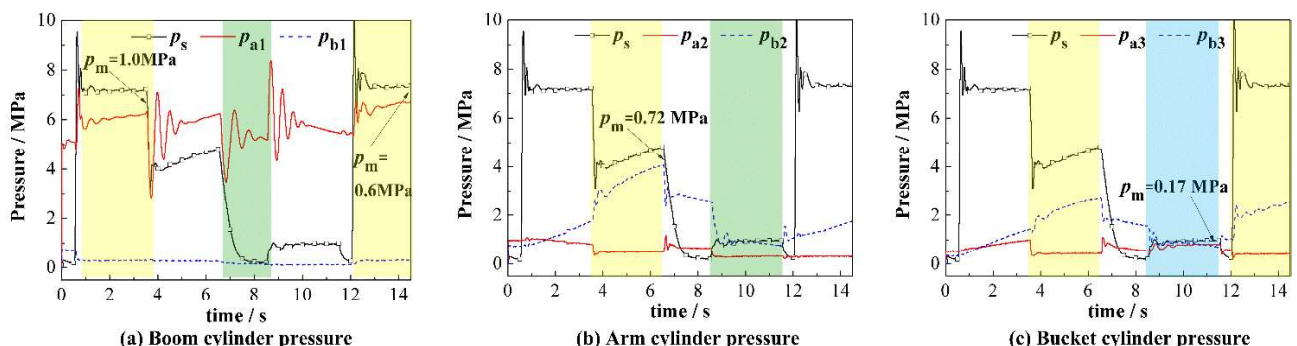
411 Following the downward trends of supply pressures and flows, the supply powers are depicted in **Fig. 21(c)**. To  
 412 analyze the energy efficiency in detail, the saved energy is also divided into three parts: decreased inlet losses,  
 413 decreased outlet losses, and regenerated potential energy.



414  
 415 **Fig.21** Comparison of supply pressure, flow, and power



416  
 417 **Fig.22** Cylinder pressure of PF\_MO mode



418  
 419 **Fig.23** Cylinder pressure of PP\_MI mode

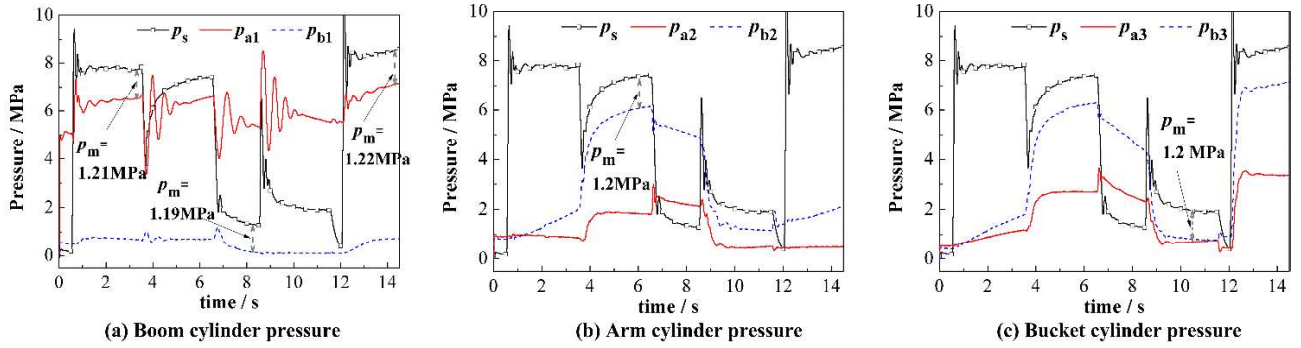


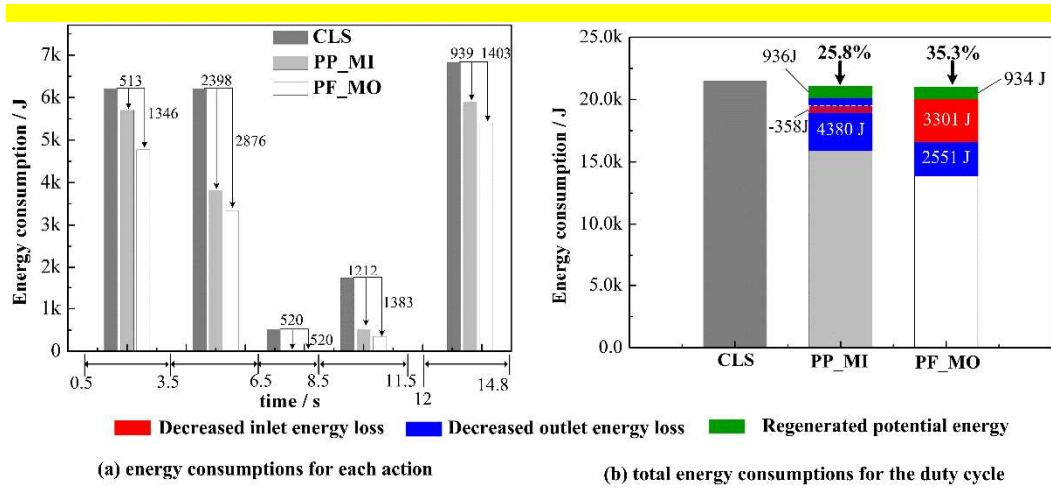
Fig.24 Cylinder pressure of CLS system

The energy consumptions for each action are given in Fig.25(a). In terms of Eqs. (1) to (6), the total energy consumptions of each hydraulic drive system for the duty cycle, as well as the saved energies of the three aspects, are depicted in Fig.25(b). Compared with the CLS system, the energy saving rates of PP\_MI and PF\_MO can reach 25.8 % and 35.3% respectively. Prominent energy improvements using the multi-mode switching are obtained. The primary contributions of energy saving are the decreases in pressure losses, which accounts for 81.1% and 86.2% of the total saved energy, respectively for PP\_MI and PF\_MO modes. The decreased outlet losses with PP\_MI mode achieve 4380 J, which are obviously larger than decreased inlet losses. In contrast, the decreased outlet losses with PF\_MO mode are lower than PP\_MI mode, but more inlet losses (3301 J) are saved, which contributes to higher efficiency. It can be explained that the energy losses with PF\_MO mode are switched from inlet to outlet. The results agree well with the theoretical analysis in Fig.15.

It is noted that the decreased inlet losses of PP\_MI are negative, which means that its inlet losses are even larger than CLS. It can be further analyzed by the energy-saving characteristics of three actuators in Fig.26. In Figs.26 (a) and (b), the outlet losses of both PP\_MI and PF\_MO modes are equal because the boom and arm are both the heavy loads during their movements and thereby their meter-out valves are both operated under pressure control modes. In Fig.26 (c), during the periods including (3.5 s~6.5 s) and (12 s~14.8 s), the bucket is the light load under NO mode. Its meter-in valve with PP\_MI mode is operated under flow control mode. Thus, the load difference between arm and bucket is dissipated in the inlet orifice of the bucket. Therefore, the decreased inlet losses with PP\_MI mode are negative. Compared with PP\_MI mode, the meter-in valve of the bucket with PF\_MO mode is fully open and its meter-out valve is operated under flow control mode. Hence, obvious decreases of inlet losses can be captured with PF\_MO, and decreased outlet losses with PF\_MO are less than PP\_MI mode. To sum up, the comprehensive reductions of pressure losses with PF\_MO are larger than that with PP\_MI for all the three actuators.

However, the saved energy by the potential energy regeneration is only in the minority of the total saved energy. It can be explained that the measuring machine is a mini-excavator, thereby the potential energy is relatively low. For a heavier machine such as 20 t excavator or crane, the saved energy by the potential energy regeneration using the

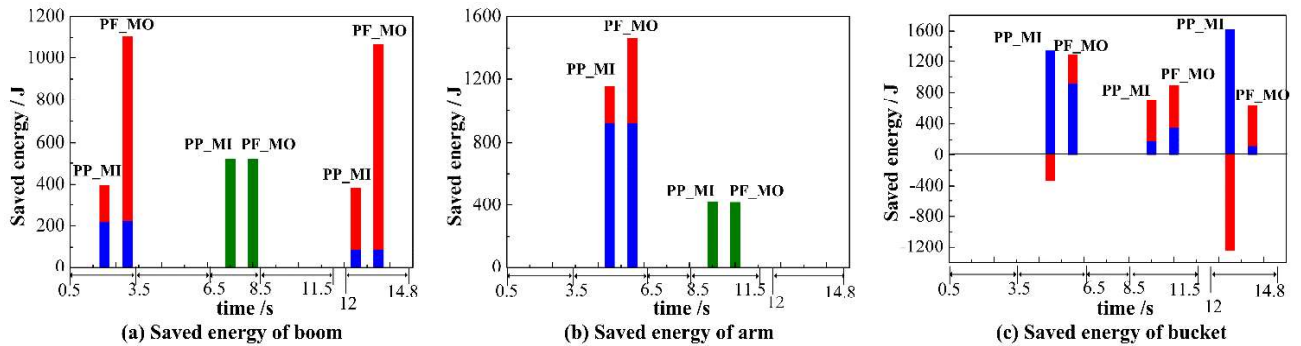
446 presented multi-mode switching method will be more remarkable.



447

448

Fig.25 Experimental results of energy consumptions



449

Fig.26 Saving energy of three actuators

450

## 451 9. Conclusions

452 This paper proposed a new methodology for multi-mode transfer of hydraulic drive system that assesses the  
 453 technological minimum of energy demand for the heavy-load mobile manipulator. The multiple modes of the cylinder,  
 454 valve, and pump are all considered using a novel designed electro-hydraulic drive system, which includes the  
 455 independent metering control valves with an electrically controlled pump. Consequently, the inlet loss, outlet loss, and  
 456 potential energy loss can be optimized simultaneously. Different mode configurations and their multi-variable control  
 457 approaches are designed to achieve two objectives including higher energy efficiency and precise motion control. The  
 458 experimental results from a duty cycle of 2 t excavator show that PP\_MI and PF\_MO control modes using the proposed  
 459 system yield 25.8% and 35.3% energy-saving ratios, respectively. Higher efficiency using PF\_MO mode can be  
 460 obtained due to the minimum inlet losses. Moreover, the motion tracking performance is not degraded by using  
 461 multi-mode switching.

## 462 Acknowledgment

463 This work was supported by the National Natural Science Foundation of China Grant (Grant No.51705152 and

464 No.91748210), NSFC-Zhejiang Joint Fund for the Integration of Industrialization and Informatization (Grant  
465 No.U1509204), Chongqing Research Program of Basic Research and Frontier Technology (Grant No.  
466 cstc2016jcyjA0253)

467 **Reference:**

468 [1] **Vukovic M, Leifeld R, Murrenhoff H.** Reducing Fuel Consumption in Hydraulic Excavators — A  
469 Comprehensive Analysis. *Energies*. 2017, 10: 687. <http://dx.doi.org/10.3390/en10050687>.

470 [2] **Wang H, Wang Q F, Hu B.** A review of developments in energy storage systems for hybrid excavators. *Automation in Construction*. 2017, 80: 1-10. <http://dx.doi.org/10.1016/j.autcon.2017.03.010>.

471 [3] **Ge L, Quan L, Zhang X, et al.** Efficiency improvement and evaluation of electric hydraulic excavator with speed  
472 and displacement variable pump. *Energy Conversion and Management*. 2017, 150: 62-71.  
473 <http://dx.doi.org/10.1016/j.enconman.2017.08.010>.

474 [4] **Axin M, Eriksson B, Krus P.** Flow versus pressure control of pumps in mobile hydraulic systems. *Proceedings of the Institution of Mechanical Engineers, Part I: Journal of Systems and Control Engineering*. 2014, 228(4): 245-256.  
475 <http://dx.doi.org/10.1177/0959651813512820>.

476 [5] **Ding R, Zhang J, Xu B, et al.** Programmable hydraulic control technique in construction machinery: Status,  
477 challenges and countermeasures. *Automation in Construction*. 2018, 95: 172-192.  
478 <https://doi.org/10.1016/j.autcon.2018.08.001>.

479 [6] **Lin J, Yeh T J.** Mode switching control of dual-evaporator air-conditioning systems. *Energy Conversion and Management*. 2009, 50: 1542-1555. <http://dx.doi.org/10.1016/j.enconman.2009.02.010>.

480 [7] **Wen H, Su B.** Hybrid-mode interleaved boost converter design for fuel cell electric vehicles. *Energy Conversion and Management*. 2016, 122: 477-487. <http://dx.doi.org/10.1016/j.enconman.2016.06.021>.

481 [8] **Wang E, Di Guo, Yang F.** System design and energetic characterization of a four-wheel-driven series – parallel  
482 hybrid electric powertrain for heavy-duty applications. *Energy Conversion and Management*. 2015, 106: 1264-1275.  
483 <http://dx.doi.org/10.1016/j.enconman.2015.10.056>.

484 [9] **Solouka A, Shakiba-Herfeh M, Arora J, et al.** Fuel consumption assessment of an electrified powertrain with a  
485 multi-mode high-efficiency engine in various levels of hybridization. *Energy Conversion and Management*. 2018, 155:  
486 100-115. <http://dx.doi.org/10.1016/j.enconman.2017.10.073>.

487 [10] **Bayomi N N, El-Maksoud R M A.** Two operating modes for turbocharger system. *Energy Conversion and Management*. 2012, 58: 59-65. <http://dx.doi.org/10.1016/j.enconman.2012.01.003>.

488 [11] **Lin T, Chen Q, Ren H, et al.** Review of boom potential energy regeneration technology for hydraulic construction  
489 machinery. *Renewable and Sustainable Energy Reviews*. 2017, 79: 358-371.  
490 <http://dx.doi.org/10.1016/j.rser.2017.05.131>.

491 [12] **Liang X, Virvalo T.** An energy recovery system for a hydraulic crane. *Proceedings of the Institution of  
492 Mechanical Engineers, Part C: Journal of Mechanical Engineering Science*. 2001, 215(6): 737-744.  
493 <http://dx.doi.org/10.1243/0954406011523983>.

494 [13] **Casoli P, Gambarotta A, Pompini N, et al.** Hybridization methodology based on DP algorithm for hydraulic  
495 mobile machinery — Application to a middle size excavator. *Automation in Construction*. 2016, 61: 42-57.  
496 <http://dx.doi.org/10.1016/j.autcon.2015.09.012>.

497 [14] **Vukovic M, Leifeld R, Murrenhoff H.** STEAM – a hydraulic hybrid architecture for excavators. *10th  
498 International Fluid Power Conference*. Dresden, Germany: 2016.

499 [15] **Xia L, Quan L, Ge L, et al.** Energy efficiency analysis of integrated drive and energy recuperation system for  
500 hydraulic excavator boom. *Energy Conversion and Management*. 2018, 156: 680-687.  
501 <https://doi.org/10.1016/j.enconman.2017.11.074>.

507 [16] **Ge L, Quan L, Li Y, et al.** A novel hydraulic excavator boom driving system with high efficiency and potential  
 508 energy regeneration capability. *Energy Conversion and Management*. 2018, 166.  
 509 <https://dx.doi.org/10.1016/j.enconman.2018.04.046>.

510 [17] **Kim H, Yoo S, Cho S, et al.** Hybrid control algorithm for fuel consumption of a compound hybrid excavator.  
 511 *Automation in Construction*. 2016, 68: 1-10. <http://dx.doi.org/10.1016/j.autcon.2016.03.017>.

512 [18] **Minav T A, Pyrhonen J J, Laurila L I E.** Permanent Magnet Synchronous Machine Sizing: Effect on the Energy  
 513 Efficiency of an Electro-Hydraulic Forklift. *IEEE Transactions on Industrial Electronics*. 2012, 59(6): 2466-2474.  
 514 <http://dx.doi.org/10.1109/TIE.2011.2148682>.

515 [19] **Minav T A, Laurila L I E, Pyrhonen J J.** Analysis of electro-hydraulic lifting system's energy efficiency with  
 516 direct electric drive pump control. *Automation in Construction*. 2013, 30: 144-150.  
 517 <http://dx.doi.org/10.1016/j.autcon.2012.11.009>.

518 [20] **Minava T A, Heikkinen J E, Pietola M.** Direct driven hydraulic drive for new powertrain topologies for non-road  
 519 mobile machinery. *Electric Power Systems Research*. 2017, 152: 390-400. <http://dx.doi.org/10.1016/j.epsr.2017.08.003>.

520 [21] **Eriksson B, Palmberg J.** Individual metering fluid power systems: challenges and opportunities. *Proceedings of  
 521 the Institution of Mechanical Engineers, Part I: Journal of Systems and Control*. 2011(225): 196-211.  
 522 <http://dx.doi.org/10.1243/09596518JSCE1111>.

523 [22] **Lu L, Yao B.** Energy-Saving Adaptive Robust Control of a Hydraulic Manipulator Using Five Cartridge Valves.  
 524 *IEEE Transaction on Industrial Electronics*. 2014, 61(12): 7046-7054. <https://doi.org/10.1109/TIE.2014.2314054>.

525 [23] **Choi K, Seo J, Nam Y, et al.** Energy-saving in excavators with application of independent metering valve.  
 526 *Journal of Mechanical Science and Technology*. 2015, 29(1): 387-395. <http://dx.doi.org/10.1007/s12206-014-1245-5>.

527 [24] **Kolks G, Weber J.** Modiciency - Efficient industrial hydraulic drives through independent metering using optimal  
 528 operating modes. *10th International Fluid Power Conference*. Dresden: 2016.

529 [25] **Nurmi J, Mattila J.** Global energy-optimised redundancy resolution in hydraulic manipulators using dynamic  
 530 programming. *Automation in Construction*. 2017, 73: 120-134. <http://dx.doi.org/10.1016/j.autcon.2016.09.006>.

531 [26] **Koivumäki J, Zhu W, Mattila J.** Energy-Efficient and High-Precision Control of Hydraulic Robots. *Control  
 532 Engineering Practice*. 2019. 10.1109/TIE.2014.2314054 10.1016/j.conengprac.2018.12.013.

533 [27] **Liu B, Quan L, Ge L.** Research on the performance of hydraulic excavator boom based pressure and flow  
 534 accordance control. *Proceedings of the Institution of Mechanical Engineers, Part E: Journal of Mechanical  
 535 Engineering*. 2017, 231(5): 901-913. <https://doi.org/10.1177/0954408916673117>.

536 [28] **Shi J, Quan L, Zhang X, et al.** Electro-hydraulic velocity and position control based on independent metering  
 537 valve control in mobile construction equipment. *Automation in Construction*. 2018, 94: 73-84.  
 538 <https://doi.org/10.1016/j.autcon.2018.06.005>.

539 [29] **Cheng M, Zhang J, Xu B, et al.** Decoupling compensation for damping improvement of the electrohydraulic  
 540 control system with multiple actuators. *IEEE/ASME Transactions on Mechatronics*. 2018, 23(3): 1383-1392.  
 541 <http://dx.doi.org/10.1109/TMECH.2018.2834936>.

542 [30] **Sheikholeslami M, Ganji D D.** Heat transfer improvement in a double pipe heat exchanger by means of  
 543 perforated turbulators. *Energy Conversion and Management*. 2016, 127: 112-123.  
 544 [http://dx.doi.org/10.1016/j.enconman.2016.08.090](https://dx.doi.org/10.1016/j.enconman.2016.08.090).

545 [31] **Sheikholeslami M, Ganji D D.** Heat transfer enhancement in an air to water heat exchanger with discontinuous  
 546 helical turbulators; experimental and numerical studies. *Energy*. 2016, 116: 341-352.  
 547 [http://dx.doi.org/10.1016/j.energy.2016.09.120](https://dx.doi.org/10.1016/j.energy.2016.09.120).